# CASE FILE COPY

# NATIONAL ADVISORY COMMITTEE FOR AERONAUTICS

TECHNICAL NOTE 3665

PERFORMANCE AND OPERATIONAL STUDIES OF A FULL-SCALE

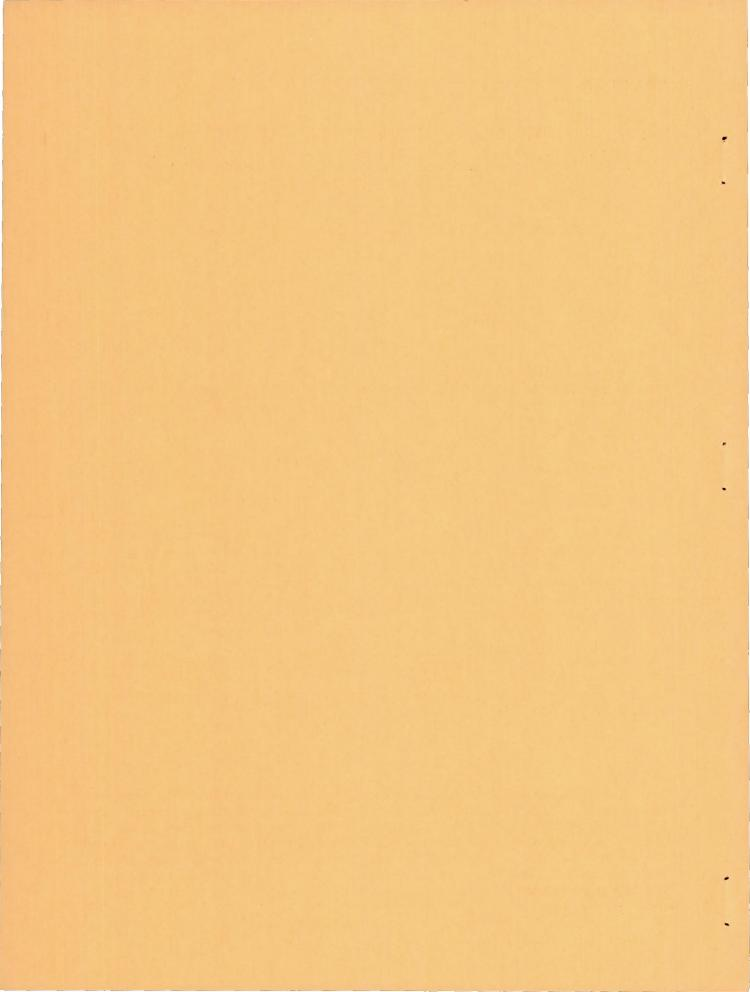
JET-ENGINE THRUST REVERSER

By Robert C. Kohl

Lewis Flight Propulsion Laboratory Cleveland, Ohio



Washington April 1956



### NATIONAL ADVISORY COMMITTEE FOR AERONAUTICS

#### TECHNICAL NOTE 3665

# PERFORMANCE AND OPERATIONAL STUDIES OF A FULL-SCALE

#### JET-ENGINE THRUST REVERSER

By Robert C. Kohl

#### SUMMARY

An axial-flow turbojet engine equipped with a hemispherical target thrust reverser was pylon-mounted beneath the wing of a cargo airplane. This thrust reverser was operated at both stationary and taxi conditions. A maximum reverse thrust amounting to 58 percent of the forward thrust was obtained at the maximum-engine-speed setting.

A truncated version of the basic hemisphere produced a reversethrust ratio approximately 5 to 8 percentage points less than that of the full-depth hemisphere.

During periods of thrust reversal, reingestion of the reversed hot gases into the engine inlet constituted an operating problem. In addition to raising the temperature levels throughout the engine, the reverse-thrust ratio was reduced by as much as 25 percentage points. Taxi tests indicated that at ground speeds of 62 knots the free-stream velocity was sufficient to disperse the reversed gas flow and prevent it from entering the engine inlet with the engine operating at maximum speed.

A maximum temperature rise of nearly 400° F above ambient was measured on a simulated wing surface located above the thrust reverser. The maximum measured rate of temperature rise on this surface was 28° F per second.

#### INTRODUCTION

The NACA Lewis laboratory has evaluated in full-scale tests the performance of a hemispherical target, which is a basic thrust-reverser type. A turbojet engine equipped with such a device was pylon-mounted under the wing of a cargo airplane, the installation simulating that on a jet bomber or transport. The thrust reverser was operated at both stationary and taxi conditions, but the airplane was not flown. In addition to obtaining the performance of the thrust reverser, the heat-rise patterns and

rates resulting from impingement of the reversed hot gases on a simulated lower wing surface were also measured. Because during stationary operation some of the hot reversed gases penetrated as far forward as the engine inlet and were reingested, taxi tests were conducted to estimate the ground speeds required to disperse the reversed gas flow and prevent reentry into the engine inlet.

In order to obtain a comparison between data obtained by the coldair model testing technique and that obtained in full scale, the full-depth hemispherical target thrust reverser and the rear portion of the engine nacelle were reproduced in quarter scale and tested on a thrust stand using unheated air. The performance obtained with the model is compared with that of the full-scale device.

The performance of a modified form of the basic hemispherical target was also obtained in full-scale tests. The modification consisted of truncating the hemisphere by means of a flat plate installed within the target. Model tests of a similar device but with different rear-engine nacelle shapes are reported in reference 1.

#### APPARATUS

An axial-flow turbojet engine, rated at 4000 pounds static sea-level thrust, was used in these experiments. The engine was suspended from the wing of a C-82 airplane. The engine and engine mounting frame together with the supporting strut were enclosed in a sheet-metal covering in order to present a streamlined impingement surface to the reverse blast and to shield the engine and reverser actuating mechanisms. The fairing which covered the supporting strut was attached to the engine cowling but was not attached to the lower surface of the wing. A photograph of the general arrangement is shown in figure 1.

The thrust reverser used for these tests consisted of a hemisphere spun from Inconel sheet. The internal diameter of the hemisphere was 24.86 inches, which closely corresponds to  $1\frac{1}{2}$  jet nozzle diameters. Cold-air model studies (ref. 1) have shown that for the hemispherical thrust reverser the  $1\frac{1}{2}$ -nozzle-diameter size represents a reasonable compromise between the improved performance of larger targets and the bulk of the target. Bulk must be considered in terms of stowage volume required at the rear of the engine.

In order to move the target in and out of the jet stream, the hemisphere was split into two equal sections. Each half of the target was attached to a pair of actuating arms that rotated through approximately

22° of arc. It was not the purpose in these experiments to simulate a flight-type stowage or actuator arrangement, but merely to provide a means for moving the target in and out of the jet blast.

The target (fig. 2(a)) was double-walled. The inner wall was relieved by a series of pressure relief holes located in the rear third of the hemisphere. The total area of the pressure relief holes represented 3 percent of the hemispherical internal surface area. Gas bled through the pressure relief holes was ducted out of the target through passages formed by the inner and outer hemisphere shells. The bled gas was discharged in a forward direction parallel to the main reversed flow. Tests were conducted with the pressure relief holes covered as well as uncovered. No significant difference in either the amount of reverse thrust or the efflux-flow pattern was observed. For the majority of the tests reported herein the bleed holes were uncovered, but no distinction is made between the runs with and without internal bleed. The doublewall construction used in the fabrication of the target offers some advantage from the standpoint of strength-weight ratio. An additional series of tests were made with a truncated version of the original hemispherical target. This modification is shown in figure 2(b).

Over-all dimensions of the installation are shown in figure 3. The target was positioned  $10\frac{1}{4}$  inches downstream of the plane of the jet noz-zle exit. This distance divided by the nozzle diameter  $(16\frac{1}{2} \text{ in.})$  is 0.621 and is called the spacing ratio.

In order to simulate the lower surface of a wing in the region of the jet exit, a temperature plate (fig. 4) 144 inches long and 72 inches wide, was suspended above the reverser as shown in figure 3. Twenty-four thermocouples were spot-welded to the inside surface of the 1/32-inch-thick stainless-steel skin in the centers of the rectangles formed by the structural stringers. The distance between the forward end of the plate and the nozzle exit plane is representative of the distance between the leading edge of the wing and the plane of the nozzle exit used in current jet pod installations. The vertical distance between the plate and the engine centerline could be altered. For these studies two positions were used: In the lower position the plate was spaced  $32\frac{1}{2}$  inches above the engine centerline; in the upper position the spacing was  $46\frac{1}{4}$  inches.

For the runs in which heat-rise rates and distribution patterns were measured on the temperature plate, the actuating arms for the hemisphere sections were positioned on the sides of the target, thus leaving the flow path between the reverser lip and the temperature plate unobstructed.

#### INSTRUMENTATION

Forward and reverse engine thrust was measured by a pair of calibrated strain-gage torquemeters. The thrust was converted to a torsional force by means of a pair of tubular thrust arms, one of which is visible in figure 1 projecting through the engine cowling. These arms formed a connecting link between the radius arms of the torquemeters and the main engine trunions. Reverse-thrust measurements include the blast forces acting on the engine cowling and support-strut fairing.

Gas temperature at the engine inlet was obtained by averaging the readings of three thermocouples equally spaced around the inlet annulus just ahead of the compressor-inlet screen. Tail-pipe temperature was measured using the standard engine thermocouple installation. Nozzle total pressure was obtained from an instrument rake located in the tail pipe just upstream of the jet nozzle. In the tests of the truncated-hemisphere configuration, the total pressure was measured in the plane of the nozzle exit by means of a single probe.

Thermocouples on the temperature plate were connected to individual temperature gages mounted on a panel that was located in the cargo compartment of the airplane. Also mounted on this panel were the three engine-inlet gas-temperature gages, an engine tachometer, and a gage that indicated the position of the reverser sections. This panel was photographed by a motion-picture camera at 8 frames per second. A time reference was supplied by a timer light mounted on the panel which flashed at 1-second intervals.

For the taxi runs the airplane ground speed was obtained by counting the number of revolutions of one of the landing-gear wheels. A cam and micro-switch follower arrangement mounted on the wheel rim caused an electrical signal to be recorded on strip film for each wheel revolution. The strip film was synchronized with the motion-picture film by a timer trace, which was energized by the same timer used on the instrument panel.

#### RESULTS AND DISCUSSION

In the following paragraphs the results obtained in these full-scale experiments are presented in terms of thrust-reverser performance. In addition, data are presented relative to some of the operating problems which arise from the use of such a device.

## Performance of Full-Depth Hemisphere

Full-scale performance. - In figure 5 the forward and reverse thrust, corrected for variations in the ambient barometric pressure, is plotted

against percentage of maximum engine speed, which is corrected for variations in the ambient inlet temperature. Reproducibility of the data is demonstrated in figure 5, where the data points shown in the plot were obtained from several test operations. Each type of symbol represents a separate operation. As will be discussed later, many of the reversethrust data points were obtained with elevated temperatures at the engine inlet. As a result, several data points obtained at maximum engine rpm appear in the plot as points at lower values of corrected engine speed.

Reverse-thrust ratio, expressed as a percentage of the corrected forward thrust at the same corrected engine speed, is shown in figure 6. Reverse-thrust ratio increases with corrected engine speed. A maximum value of 58 percent was obtained at a corrected engine speed of 100 percent of maximum rpm. This value, however, does not represent the best possible performance attainable with the hemisphere target. Model tests of the  $1\frac{1}{2}$ -nozzle-diameter hemisphere with unrestricted weight flow (ref. 1) show that the optimum reverse-thrust ratio is about 63 percent at nozzle pressure ratios between 2.4 and 3.0. The engine used for these tests does not produce a nozzle pressure ratio sufficiently high to achieve the higher reverse-thrust ratios reported in the reference.

The nozzle pressure ratio produced by the engine during the stationary tests is plotted against corrected engine speed in figure 7. The data points again represent a compilation of measurements obtained in several stationary test operations. The peak nozzle pressure ratio is 1.78 at a corrected engine speed of 100 percent of maximum rpm.

If the relation between nozzle pressure ratio and engine speed is known, the reverse-thrust ratio can be cross-plotted as a function of nozzle pressure ratio (see fig. 8). This is the variable used in reporting the model test results. The reverse-thrust ratio increases with nozzle pressure ratio.

Comparison between full-scale and model performance. - A direct comparison of the model and full-scale reversal data (fig. 9) shows that, for the same spacing ratio, the model produced about 4 to 8 percentage points higher reverse-thrust ratio. The general trend of the two performance curves is the same. The lower reverse-thrust ratio produced by the full-scale target may be partly attributed to the leakage along the parting line of the two hemispherical half-sections. In the model tests the target consisted of a single piece and had no such parting line through which leakage could occur.

Effect of thrust reverser on engine operation. - Unless precautions are taken in the design of a thrust reverser, the weight flow through the engine may be restricted, particularly at the lower engine speeds. If the fuel flow is maintained constant, restriction of the engine air flow

can result in compressor stall and overheating of the turbine and exhaust systems. Reducing the fuel flow as a corrective measure will decrease the reverse thrust available for braking. For a target of a given size there is a minimum distance between the jet nozzle and the target below which the weight flow will be restricted. This distance is usually expressed in terms of spacing ratio. The effect of spacing ratio (see fig. 3) on the engine weight flow has been investigated using reduced-scale cold-air models (ref. 1). These tests indicated that a spacing ratio of 0.621 would be more than sufficient to avoid weight-flow restriction. The spacing ratio of 0.621 was used in the full-scale tests.

Because weight flow was not measured in the full-scale tests, the engine nozzle pressure ratio or the over-all engine temperature ratio may be used to determine the presence of blockage. If blockage is present, the pressure-ratio and temperature-ratio values will be higher than for the case where there is no blockage. Over-all engine temperature ratio is plotted against corrected engine speed in figure 10. The solid symbols represent data obtained with the thrust reverser in operation. The open symbols represent data obtained with the thrust reverser in the open position and, in some cases, completely removed from the engine. Regardless of whether the reverser was operative or inoperative, all data points tend to cluster about an average operating line. The lack of demarcation between operation with and without thrust reversal is taken to mean that the engine weight flow was not reduced during reverse thrust.

Thrust-reverser discharge-flow angle. - The variation of reverse-thrust ratio with nozzle pressure ratio depends largely upon the angle through which the gas is turned by the thrust-reversing device. In the full-scale tests a flow survey was made in which the turning angle of the reversed gas was measured. The survey rake used for this study is shown in figure 11. Each tube in the survey rake was directed at the same point on the lip of the hemisphere. All tubes were located in the same horizon-tal plane at a radius of  $1\frac{1}{2}$  nozzle diameters from the target lip. The variation of turning angle with nozzle pressure ratio is shown in figure 12. The survey also indicates that the flow discharges from the thrust reverser in the form of a conical sheet. The turning angle increases with nozzle pressure ratio. For example, at a nozzle pressure ratio of 1.43 the average turning angle is about  $120^{\circ}$ , whereas at a nozzle pressure ratio of 1.69 the average turning angle has increased to about  $143^{\circ}$ .

Visual observation during periods of reverser operation revealed that at nozzle pressure ratios above approximately 1.40 the discharge flow adhered to the rear fairing as far forward as the cylindrical midsection of the engine cowling (see fig. 3), and ultimately turned through  $180^{\circ}$ . At the cylindrical midsection the reversed flow appeared to be confined within an annular envelope about 4 feet thick.

NACA TN 3665 7

A tendency for the reversed flow to adhere to the rear fairing and forward portions of the engine cowling was observed in both the scale-model and full-scale experiments. In the model tests at nozzle pressure ratios above 1.8, the reversed flow adhered to the external fairing. Altering the spacing ratio of the model from 0.438 to 1.000 had no noticeable effect on the tendency of the flow to adhere to the external fairing.

The rear fairing used in the full-scale tests had high angles with respect to the engine centerline as well as a large projected area. Such a configuration can have a marked effect on the reverse-thrust ratio. For this reason the rear fairing on the full-scale engine was duplicated on the scale model. Tests with the scale model showed that subambient pressures are produced on the rear fairing during reverse-thrust operation when the reversed flow adheres to this surface. If the projected area of the rear fairing is relatively large with respect to the jet-nozzle area, as it is for the configuration reported herein, and if the reversed flow adheres to this surface and is turned to a more forward direction, a suction is produced on the rear fairing that contributes to the thrust-reversal obtained. The blunt rear fairing produced 10 to 14 percentage points of additional reverse-thrust ratio as compared with the results obtained with the models having more streamlined rear-fairing shapes reported in reference 1.

# Operational Problems

Reentry of reversed gas into engine inlet. - In the full-scale tests the tendency of the reversed flow to cling to the cowling constituted an operational problem. Forward movement of the reversed gas was observed as far as 20 to 30 nozzle diameters ahead of the nozzle exit when the airplane was standing still. When the hot exhaust gases penetrated ahead of the engine, some of the exhaust gases were drawn into the engine inlet. This condition is referred to as "reingestion." During periods of reingestion, the engine-inlet gas temperature increases rapidly. Without remedial action, the operating temperature levels throughout the engine can be raised substantially beyond the safe limits.

Some concept of the rate of inlet temperature rise can be obtained from figure 13, which shows the time histories of a series of typical reverse-thrust operations. The inlet temperature rise above ambient temperature is plotted against time, in seconds, for four engine tachometer speed settings. Zero time in each case corresponds to the instant at which the hemisphere half-sections reached the full-closed position. The rate of inlet temperature rise was highest as the thrust reverser was closing. The maximum rate of inlet temperature rise was about 69° F per second and occurred at maximum engine speed. Lesser rates of temperature rise occurred at lower engine tachometer speed settings. At 60 percent of maximum engine rpm a rate of 20° F per second was obtained. Because

of reingestion the temperature levels throughout the engine, including the temperature at the nozzle exit, continued to increase, but at a somewhat reduced rate after the thrust reverser was fully closed. A condition of temperature instability was established where the engine-inlet gas temperature increased as a result of the higher exhaust temperature while the exhaust temperature was increasing because of the higher inlet temperature. No upper limit to this cyclic temperature rise was found. Unless checked, such a condition could lead to destruction of the engine. On several occasions inlet temperatures above 300° F were observed, and in one instance, an inlet temperature of 350° F was reached before the thrust reverser was opened. Normally, the inlet temperature was permitted to increase until an arbitrary limit of 200° F was reached, whereupon the thrust reverser was opened. Start of the opening is indicated by an arrow on each of the curves in figure 13.

The reverse-thrust ratio is reduced during periods of reingestion. The effect of engine-inlet temperature on reverse-thrust ratio is generalized in figure 14. The reverse-thrust term is obtained from figure 5 for the values of the engine tachometer speed setting shown as the parameter in figure 14 and corrected for the engine-inlet gas temperatures listed along the abscissa of figure 14. As was mentioned previously, many of the reverse-thrust data points plotted in figure 5 were obtained during periods of reingestion when the engine-inlet temperatures were above ambient. The forward-thrust term is obtained directly from figure 5 for each of the engine tachometer speed settings shown as the parameter in figure 14. It can be seen from figure 14 that at the maximum engine tachometer speed settings the reverse-thrust ratio decreases from 58 percent at an inlet temperature of 60° F to 33 percent at an inlet temperature of 200° F, a loss of 25 percentage points. The reduction in reverse-thrust ratio is attributed to the decrease in engine-inlet gas density and the lowered performance of the compressor, combustor, and turbine components. At a given throttle setting the engine fuel pressure was controlled by a governer that sensed rotational speed only. The engine maintained a constant mechanical speed through periods of reingestion, but the component performance varied with the corrected rotational speed and therefore changed with engine-inlet gas temperature.

Taxi tests. - A series of taxi runs were made to determine the free-stream velocity required to prevent reingestion of the reversed gas flow. The airplane was accelerated using the reciprocating engine on the left wing together with the jet engine on the right wing. The length of the runway available for accelerating and stopping determined the peak airplane speed attainable.

At the higher jet-engine tachometer speed settings it was possible to reach a maximum ground speed of about 74 knots with sufficient margin of runway remaining to bring the airplane to a stop using the thrust reverser and wheel brakes. As the airplane reached its maximum ground

NACA TN 3665

speed, the data-recording apparatus was started and the thrust reverser was closed. The reverser remained closed and the airplane speed decreased until reingestion raised the temperature at the engine inlet to 200° F, whereupon the target was opened. Taxi runs were made at jet-engine tachometer speed settings of 75, 90, and 100 percent of maximum engine rpm. The taxi tests were conducted at times when the prevailing winds were light and variable so that the measured ground speed is considered to be the free-stream velocity.

The effect of ground speed on reingestion is shown in figure 15, where engine-inlet gas temperature is plotted against ground speed. The figure shows the time histories of three separate taxi runs, each run at a different jet-engine tachometer speed setting. The time history begins at the higher ground speed and progresses from left to right. The position of the reverser at all times during the sequence is indicated. In addition, the elapsed time from the start of full thrust-reverser closure is shown in seconds. These taxi runs demonstrated that for each jet-engine tachometer speed setting there is a minimum free-stream velocity that will prevent reingestion. At maximum jet-engine speed this critical velocity is shown to be about 62 knots decreasing to 37 knots at 75 percent of maximum rpm. When reingestion begins, however, the inlet temperature climbs steadily until the thrust reverser is opened.

Reingestion is particularly troublesome because of the loss of reverse-thrust ratio that accompanies it. According to figure 15, this loss of reverse-thrust ratio occurs during the latter portion of the landing roll where aerodynamic-type speed-reduction devices, such as flaps and drag chutes, become ineffective and the aircraft depends heavily on the thrust reverser and wheel brakes for stopping. The inlet-gastemperature data obtained during the taxi tests were used in conjunction with figure 14 to determine the loss of reverse-thrust ratio that accompanied the inlet temperature rise. The deterioration of reverse-thrust ratio that occurred with the rise of the engine-inlet temperature is illustrated in figure 16, where the reverse-thrust ratio is plotted against ground speed for three engine tachometer speed settings. Superimposed on the curves is an elapsed-time scale. Elapsed time from the instant of complete target closure is shown in seconds. The reversethrust ratio is diminished by as much as one-half during the run at the maximum engine tachometer speed setting. At the lower ambient temperatures that accompany icy-runway conditions, the reversed-gas temperatures at the engine inlet may be reduced somewhat, but it is doubtful whether the losses of reverse-thrust ratio of the magnitude shown in figure 14 would be overcome completely.

Heating of adjacent surfaces by reversed engine exhaust. - Another phase of this investigation dealt with the heating effect of the reversed blast on aircraft surfaces in the vicinity of the thrust reverser. The lower surface of a wing adjacent to the pylon-mounted engine was simulated by the temperature plate shown in figures 3 and 4.

10 NACA TN 3665

Time histories of the temperature-rise pattern on the simulated lower wing surface show that the temperature rise was greatest on the area forward of the jet-nozzle-exit plane for all engine-operating conditions, including taxi operation. The observed temperature rise was greatest at a position 39 inches forward of the jet-nozzle-exit plane and tended to be symmetrical about the longitudinal centerline of the temperature plate. Time histories of the temperature rise as measured at a position 39 inches forward of the jet-nozzle-exit plane and 9 inches outboard of the longitudinal centerline of the temperature plate are shown in figure 17 for two positions of the temperature plate above the engine. The symbols represent data obtained with the airplane standing still with only moderate (5 to 10 knots) surface winds. The lines represent data measured during the deceleration periods of the taxi runs. Again, the time scale is referenced to the instant of complete target closure. The temperature-rise value at the start of each run varies somewhat because the plate was not completely cooled to ambient temperature between each run. The maximum temperature rise shown in each case represents the value that existed at the time the maximum allowable temperature (200° F) was being reached at the engine inlet. The temperature on the plate begins to decay as soon as the target is opened. The start of this decay can be seen in some of the runs. The thermal conductivity of the material used in an actual wing, together with structural bulk concentration, can be expected to affect the heat-rise rate somewhat.

The effect of air flow during airplane taxying is obtained from a comparison of the temperature-rise data obtained during stationary operation with that measured during the taxi runs. A slightly greater temperature-rise rate is indicated when an external velocity field is present to divert the thrust-reverser discharge flow so that a greater amount of impingement of hot gas occurs on the test surface. The data obtained in these tests indicated a maximum temperature-rise rate of 280 F per second and an average temperature-rise rate of 10° to 20° F per second of continuous operation. The rate is roughly proportional to the engine tachometer speed setting. The maximum rate of heat transfer to the plate was on the order of 4 Btu per second per square foot. This maximum occurred at the following conditions: maximum engine rpm; plate temperature, 205° F; engine-nozzle-exit temperature, 1247° F; temperature plate located  $32\frac{1}{2}$  inches above engine centerline; airplane ground speed, 68 knots. The rate of heat transfer to the plate at the various stations is approximately equal to the product of skin specific heat, skin weight per unit area, and the rate of temperature rise. The effect of heat conduction to the stringers within the plate on the surface temperature was computed to be small.

Patterns of the temperature distribution on the lower surface of the temperature plate are shown in figure 18 for three engine tachometer speed settings. The data are presented as the difference between the observed

temperature and the prevailing ambient temperature. Figures 18(a) and (b) show the results obtained during both stationary and taxi operations where the test surface was positioned  $46\frac{1}{4}$  inches above the engine centerline, and figures 18(c) and (d) show the equivalent data for the case where the test surface was positioned  $32\frac{1}{2}$  inches above the engine centerline. Because a bomber or transport-type aircraft equipped with a jet reversal device would require about 15 seconds of reverse-thrust operation during the landing roll, each pattern in figure 18 gives the temperature distribution after 15 seconds of full thrust reversal. Surface heating is largely confined to the forward third of the plate area (fig. 4). There is a slight rearward shift of the contours during the taxi operations that is accompanied by a small increase in the peak temperature rise. A maximum temperature rise of nearly 400° F above ambient occurred during the taxi run at maximum engine speed with the temperature plate in the lower position. A temperature rise of this magnitude might preclude the use of aluminum or magnesium structure in the areas likely to come in contact with the reversed hot gases.

# Performance of Modified Hemisphere

In the reduced-scale-model tests of the hemisphere (ref. 1) several modifications of the basic shape were tested. These modifications included the installation of a flat plate normal to the thrust line at various depths within the hemisphere. Model tests indicated that the performance penalties were not large. An arrangement of this sort was tested in full scale. The target, however, was spaced a little farther behind the nozzle-exit plane in the full-scale tests. The target configuration is shown in figure 2(b). For these tests the modified thrust reverser was not actuated. Therefore, the time-history data of the temperature distribution on the simulated wing surface were not obtained.

The corrected thrust characteristic of the modified thrust reverser is plotted against corrected engine speed in figure 19. The reverse-thrust developed by the shallower target is somewhat less than that produced by the full-depth hemisphere (fig. 5). The peak value of reverse-thrust ratio is 52 percent at maximum corrected engine speed and a nozzle pressure ratio of 1.84. The relation between reverse-thrust ratio and engine speed for the modified reverser (fig. 20) and the relation between reverse-thrust ratio and nozzle pressure ratio (fig. 21) reflect the reduced values, amounting to between 5 and 8 percentage points of reverse-thrust ratio at the higher engine speeds and nozzle pressure ratios.

The reduction in reverse-thrust ratio with the truncated hemisphere is attributed, for the most part, to the smaller angle through which the flow is turned. Target efflux-flow-angle surveys for several engine

nozzle pressure ratios are shown in figure 22. When compared with the discharge-angle surveys for the full-depth hemisphere (fig. 12), the patterns obtained with the truncated hemisphere show that the turning angle has been reduced by 5° at the lower nozzle pressure ratios to 25° at the higher nozzle pressure ratios.

At the lower engine speeds, the truncated hemisphere caused a reduction in the weight flow through the engine. Evidence of this can be seen in the engine-nozzle-pressure-ratio characteristic shown in figure 23. Blockage, which causes a rise in the nozzle pressure ratio, is indicated at engine speeds up to 85 percent of maximum rpm. Similarly, a higher over-all engine temperature ratio (not shown) was obtained over the same engine-speed range. These data verify the results of model tests of several target configurations (ref. 1) where the weight-flow reduction became increasingly severe as the nozzle pressure ratio was lowered. The blockage encountered in these tests, however, was not severe enough to cause any noticeable compressor surge or turbine overheating.

#### SUMMARY OF RESULTS

This investigation of a full-scale target-type hemispherical thrust reverser produced the following results:

- 1. The reverse-thrust ratio increased with corrected engine speed and nozzle pressure ratio. The maximum reverse-thrust ratio obtained was 58 percent with the full-depth hemispherical target at maximum corrected engine speed and a nozzle pressure ratio of 1.78.
- 2. Reverse-thrust ratio obtained in the full-scale tests of the full-depth hemisphere was 4 to 8 percentage points less than that obtained in tests of the quarter-scale cold-air models of the same configuration. The reduction is attributed, in part, to gas-flow leakage along the parting line of the actuated full-scale target.
- 3. When the airplane was stationary, closing the thrust reverser caused reingestion of the reversed hot gases. During periods of reingestion the engine-inlet temperature increased to the extent that the reverse-thrust ratio was reduced from 58 to 33 percent at maximum engine speed. Taxi tests indicated that reingestion is abated at a ground speed of 62 knots, at the maximum engine speed.
- 4. The temperatures measured on the lower surface of a simulated wing located  $32\frac{1}{2}$  inches above the engine centerline indicate a maximum temperature rise of nearly  $400^{\circ}$  F, and a maximum rate of rise of  $28^{\circ}$  F per second during reverse-thrust operation.

NACA TN 3665

5. A truncated version of the basic hemispherical configuration produced a peak thrust reversal of 52 percent at maximum corrected engine speed and a nozzle pressure ratio of 1.84, which was approximately 5 to 8 percentage points less than that of the full-depth hemisphere. Some weight-flow blockage was detected at the lower nozzle pressure ratios, but the effect on engine operation was not serious.

Lewis Flight Propulsion Laboratory
National Advisory Committee for Aeronautics
Cleveland, Ohio, January 19, 1956

# APPENDIX - SYMBOLS

The following symbols are used in this report:

- A distance between engine centerline and lower surface of temperature plate
- d diameter
- axial distance between nozzle exit and lip of hemisphere
- P total pressure
- p static pressure
- T temperature

# Subscripts:

- a ambient
- b barometric
- i engine inlet
- n nozzle
- o observed
- t tail pipe

# REFERENCES

1. Steffen, Fred W., McArdle, Jack G., and Coats, James W.: Performance Characteristics of Hemispherical Target-Type Thrust Reversers. NACA RM E55E18, 1955.

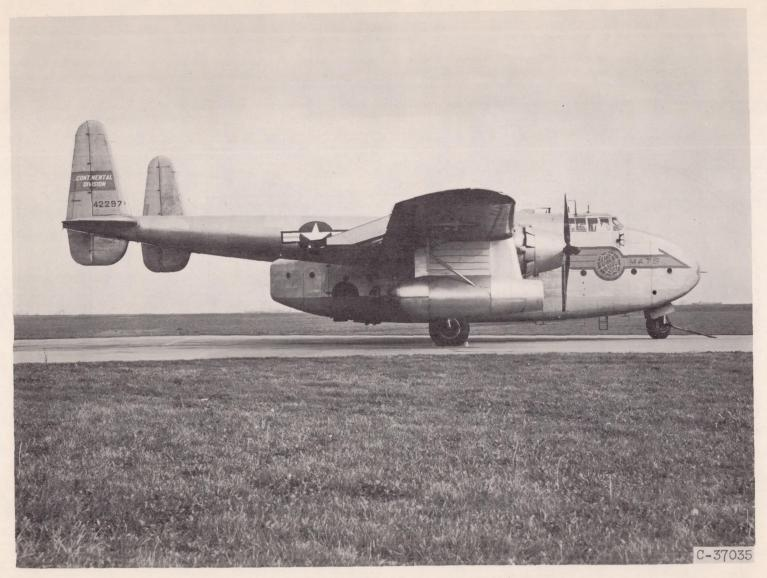


Figure 1. - Full-scale hemisphere thrust-reverser installation.

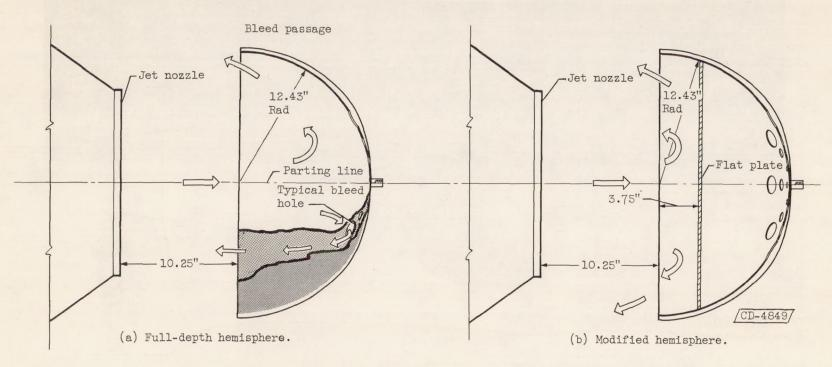


Figure 2. - Target configurations used in full-scale thrust-reverser investigation.

· CE-3

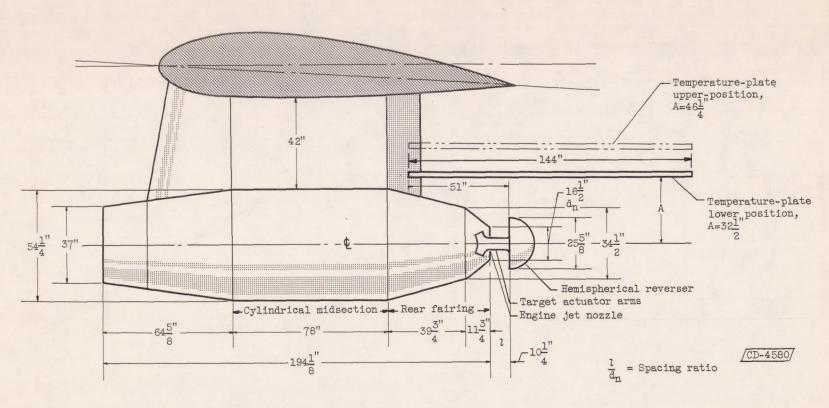


Figure 3. - General arrangement of full-scale experimental thrust-reversal apparatus.

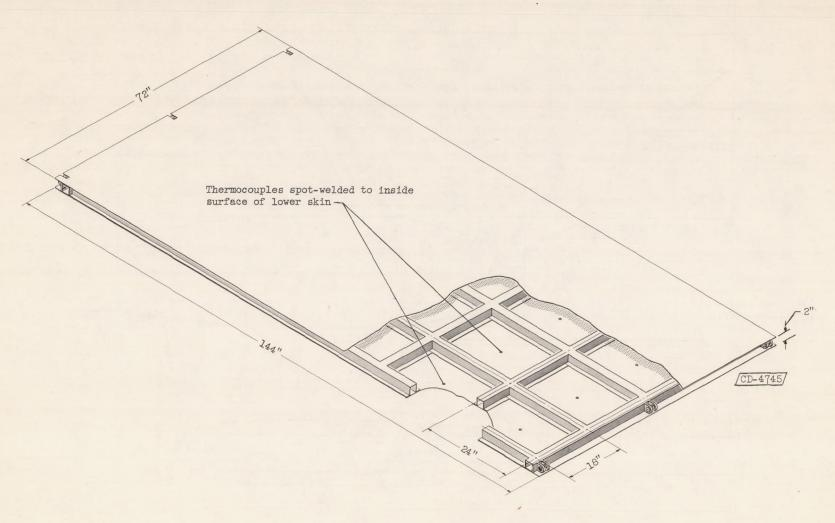


Figure 4. - Temperature plate used to simulate lower surface of airplane wing.

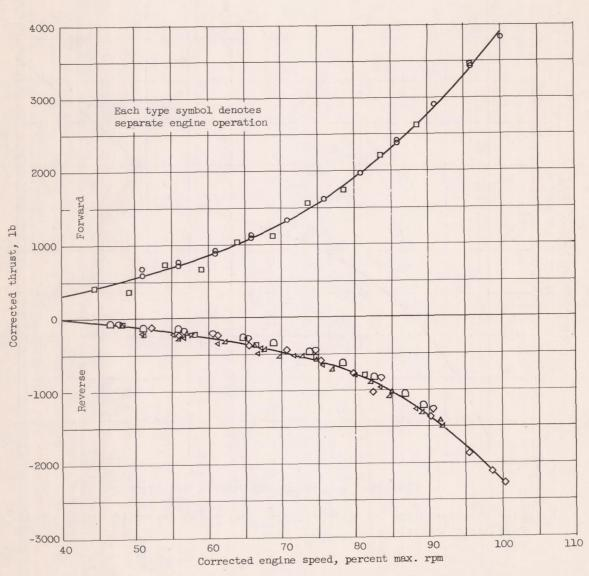


Figure 5. - Variation of forward and reverse thrust with corrected engine speed. Full-depth hemisphere.

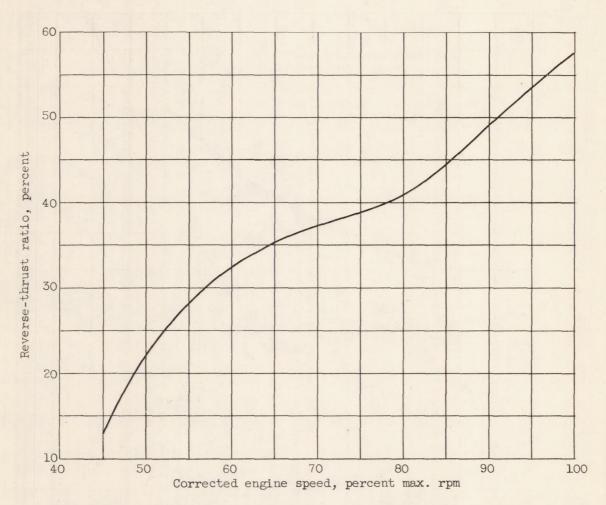


Figure 6. - Variation of reverse-thrust ratio with corrected engine speed. Full-depth hemisphere.

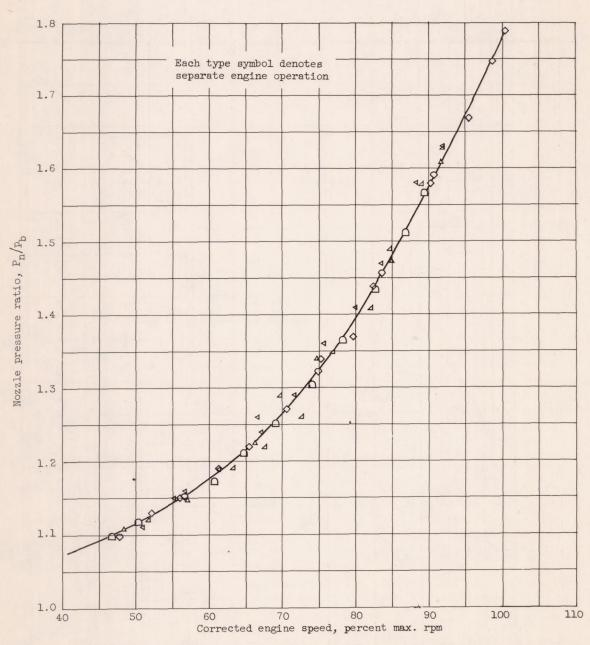


Figure 7. - Variation of nozzle pressure ratio with corrected engine speed obtained in stationary tests. Forward and reverse thrust; full-depth hemisphere.

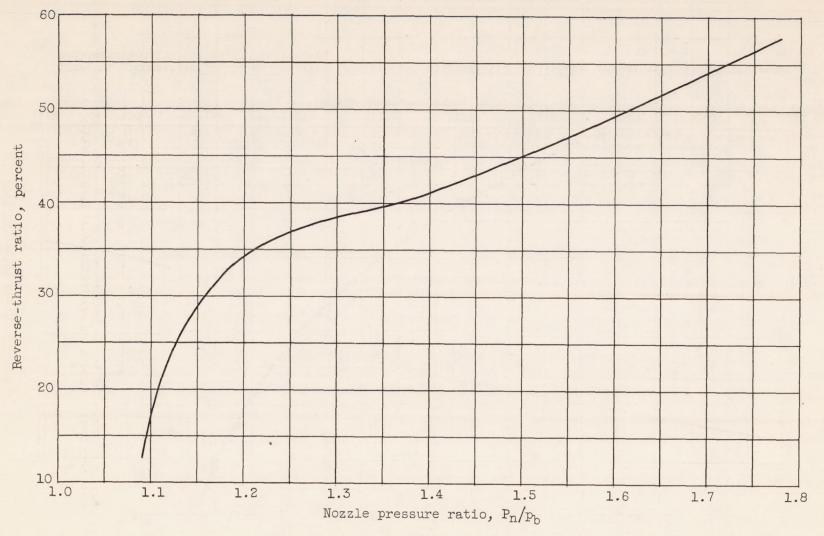


Figure 8. - Variation of reverse-thrust ratio with nozzle pressure ratio. Full-depth hemisphere.

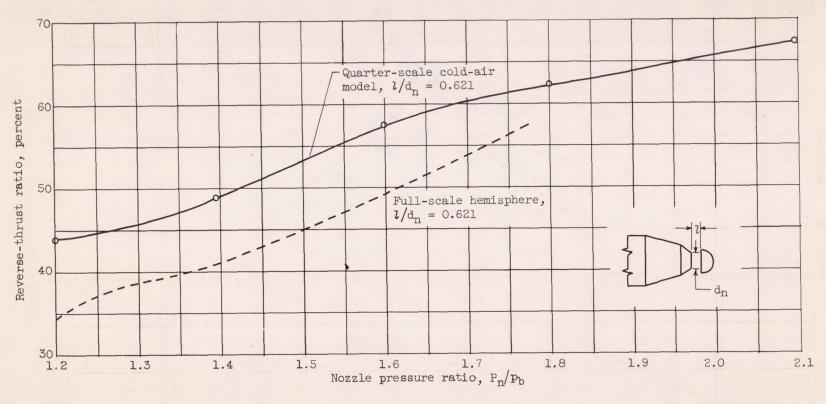


Figure 9. - Comparison of thrust-reverser performance obtained with full-scale hemisphere and quarter-scale cold-air model. Full-depth hemisphere.

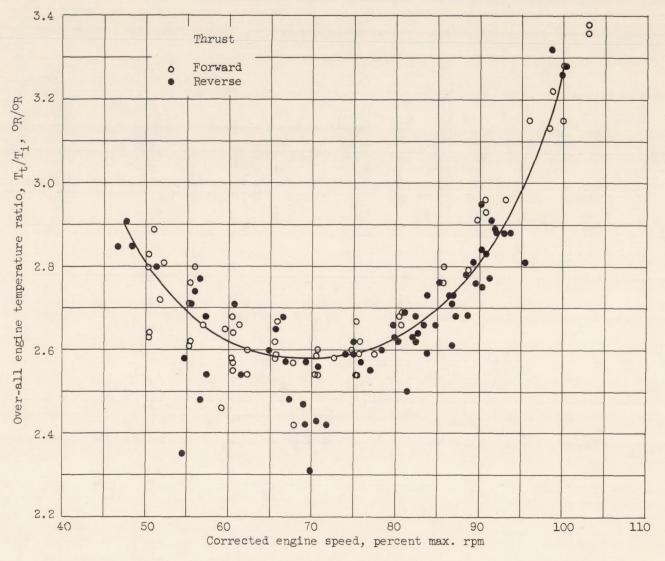


Figure 10. - Summary of engine over-all temperature ratio with and without reverse thrust. Full-depth hemisphere.

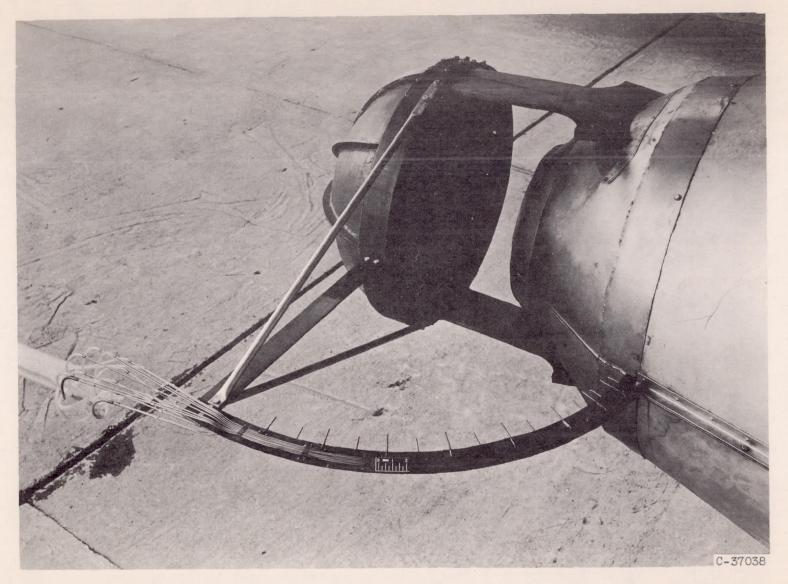


Figure 11. - Installation of survey rake for measurement of reverser discharge-flow angle.

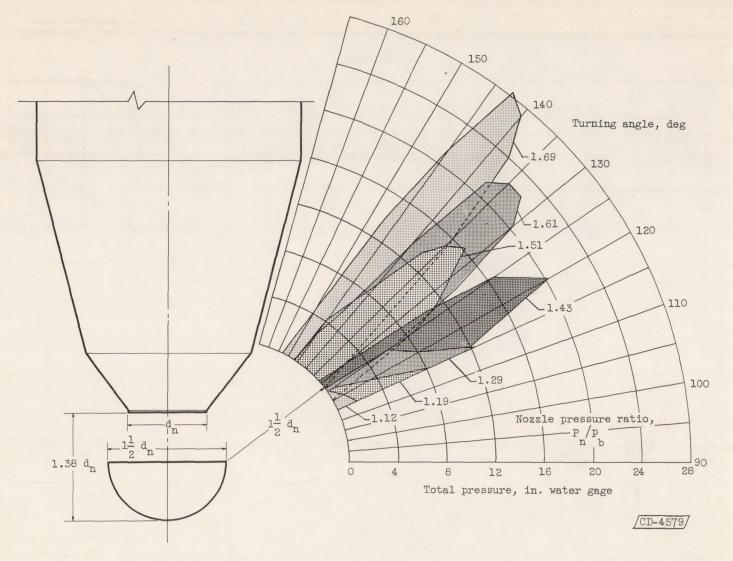


Figure 12. - Variation of thrust-reverser discharge-flow angle with nozzle pressure ratio. Full-depth hemisphere.

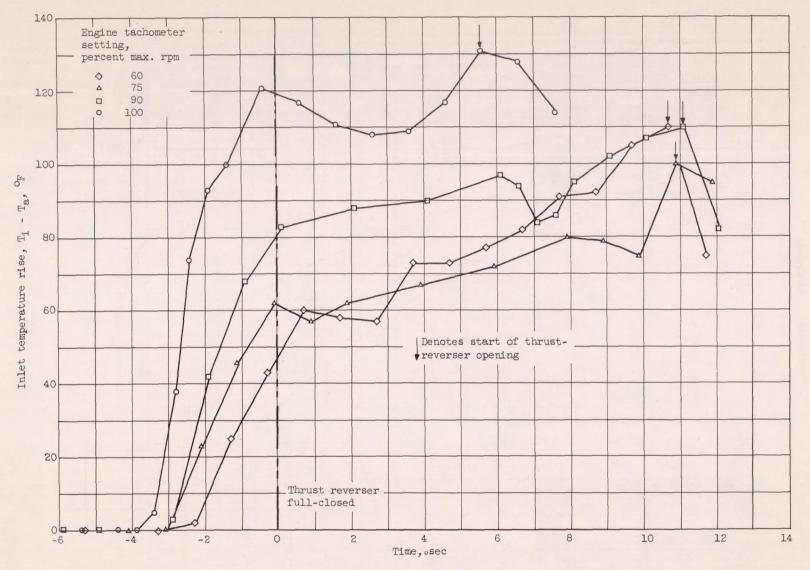


Figure 13. - Engine-inlet gas-temperature rise resulting from reingestion of reversed gases. Full-depth hemisphere; stationary operation.

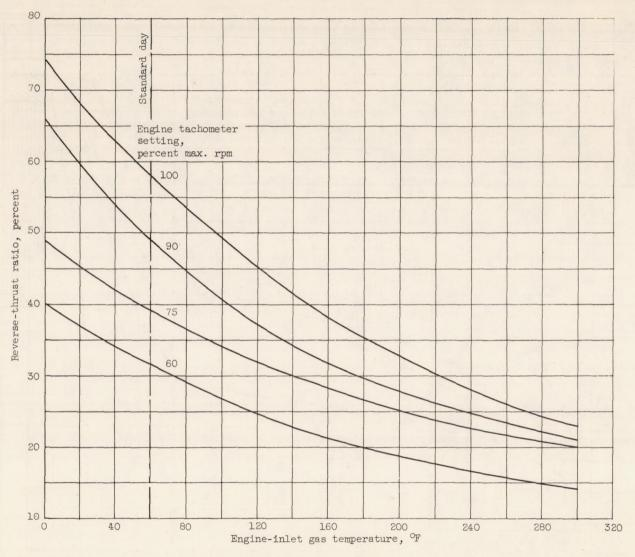


Figure 14. - Effect of engine-inlet gas temperature on reverse-thrust ratio available for braking. Full-depth hemisphere.

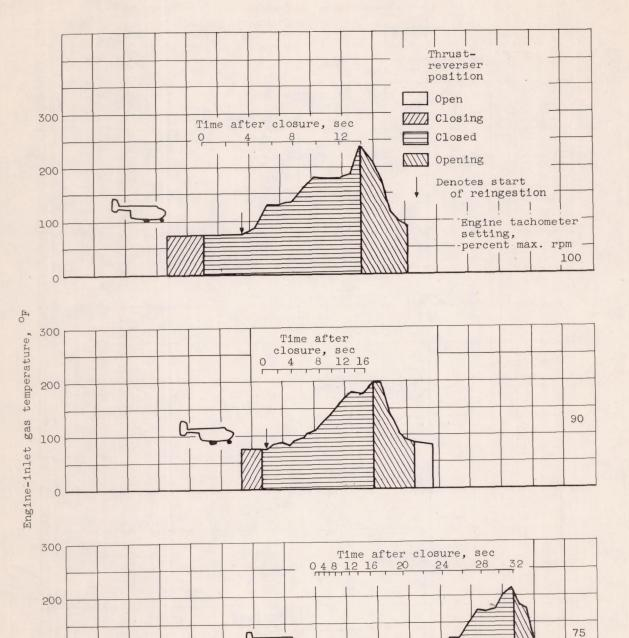


Figure 15. - Effect of airplane ground speed on engine-inlet gas temperature resulting from reingestion of reversed gases.

Ground speed, knots

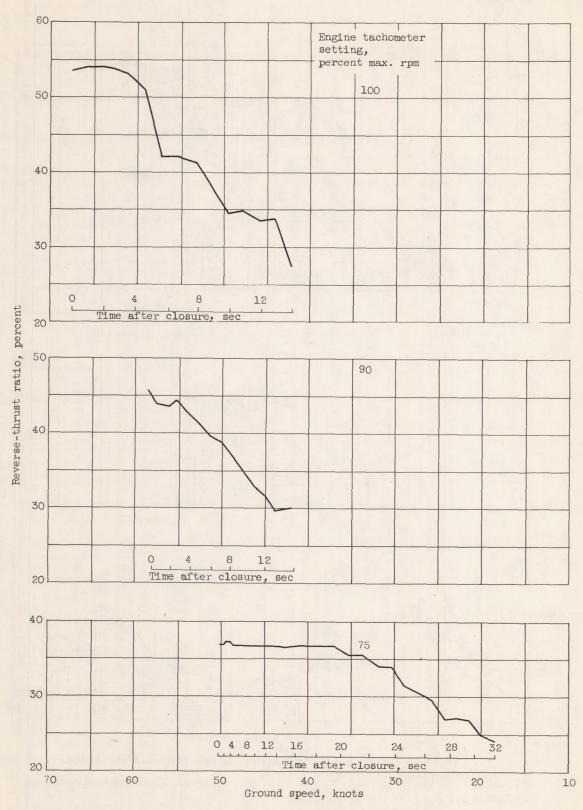
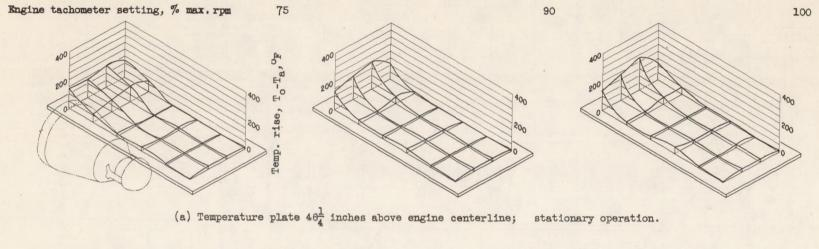


Figure 16. - Effect of airplane ground speed on reverse-thrust ratio. Full-depth hemisphere.

(b) Temperature plate  $32\frac{1}{2}$  inches above engine centerline.

Figure 17. - Maximum temperature rise measured on simulated-wing lower surface. Full-depth hemisphere.



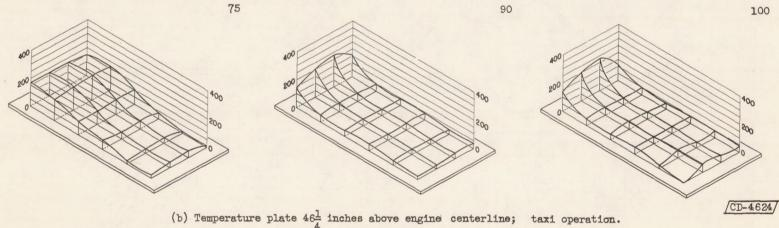
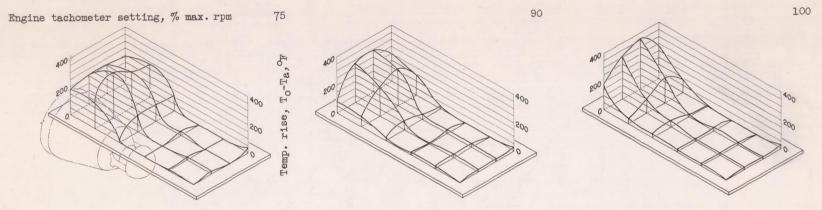
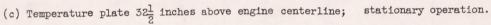


Figure 18. - Temperature patterns produced on simulated-wing lower surface after 15 seconds of full reverse thrust. Full-depth hemisphere.





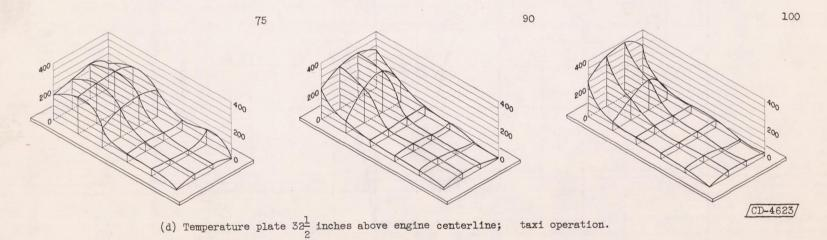


Figure 18. - Concluded. Temperature patterns produced on simulated-wing lower surface after 15 seconds of full reverse thrust. Full-depth hemisphere.

NACA TN 3665

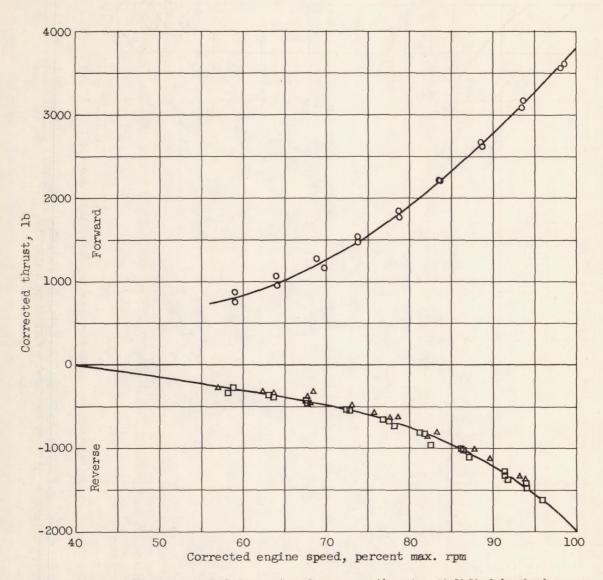


Figure 19. - Corrected forward and reverse thrust. Modified hemisphere.

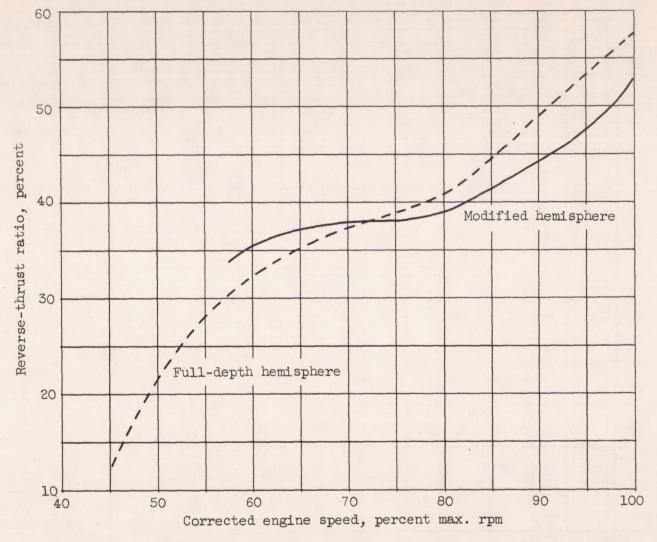


Figure 20. - Comparison of reverse-thrust ratio with engine speed. Full-depth and modified hemispheres.

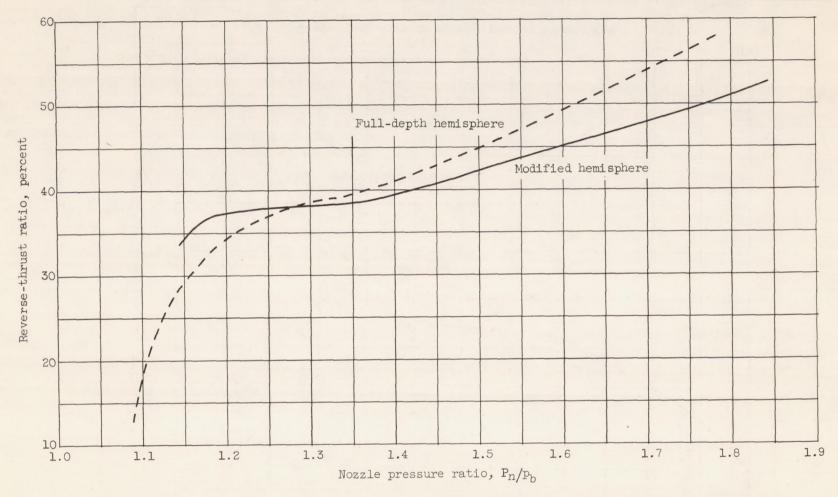


Figure 21. - Comparison of reverse-thrust ratio with nozzle pressure ratio. Full-depth and modified hemispheres.

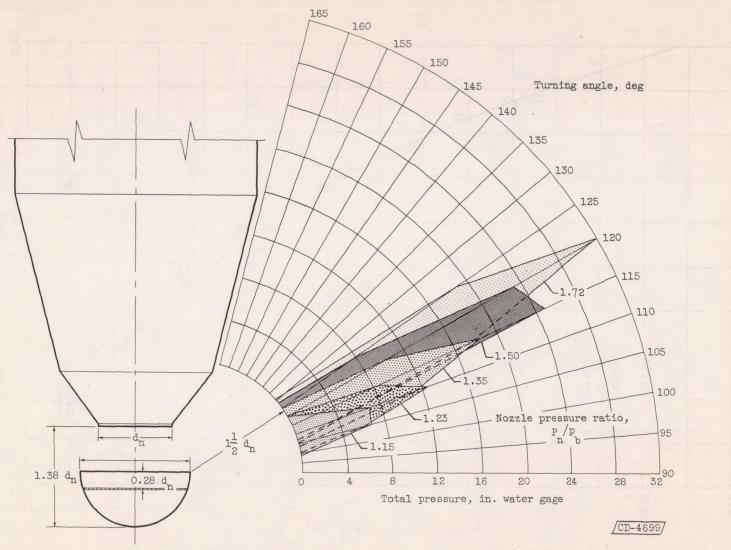


Figure 22. - Variation of thrust-reverser discharge-flow angle with nozzle pressure ratio. Modified hemisphere.

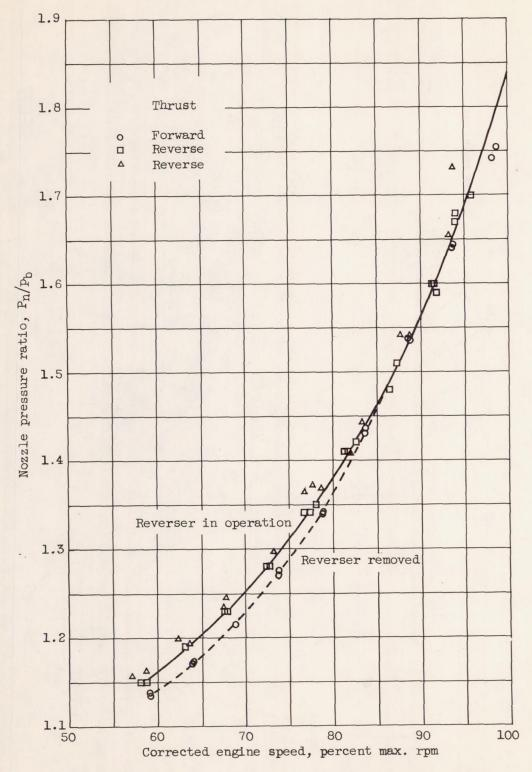


Figure 23. - Relationship of nozzle pressure ratio to engine speed for turbojet engine with and without modified hemisphere reverser.